GPS + GLONASS CORS Processing: The Asian-Pacific APREF Case

A. Nardo, L. Huisman, and P.J.G. Teunissen

Abstract

The ongoing completion of the GLONASS system asks for a new assessment of its performance in relation to CORS network processing. The recent established Asian-Pacific Reference Frame (APREF) offered such an opportunity. Daily double-difference network solutions have been computed both for GPS-only and GPS + GLONASS processings. The formal precision of the daily solutions as well as the time series of the coordinates and reference frame parameters, derived from multi-annual combinations (2.5 years) of the daily solutions, have been used to assess the effect of the additional GLONASS observations on the estimates of the coordinates and the stability of the reference frame. Results show that, for 24-h data batches, GLONASS adds little improvement when compared to GPS-only processing.

Keywords

GPS • GLONASS • CORS • ITRF • REFERENCE FRAME

1 Introduction, Motivation and Goals

The Asian-Pacific Reference Frame (APREF[1]) is a joint initiative to create and maintain a large geodetic network for supporting a wide field of applications and studies (positioning, navigation, geodynamics, climatology, space weather). As the networks of the North American Reference Frame (NAREF) and the European Reference Frame (EUREF), the Asian-Pacific APREF network also constitutes of several hundreds regionally deployed GNSS receivers. Usually the data processing for such networks is based on double differenced phase observables and daily observation time spans. As the APREF network is still being built, its density cannot be compared with the NAREF and EUREF counterparts. The average baseline length decreases as soon as new receivers become active, but the APREF network is spread over a wider region, separated by the Pacific and Indian oceans. For this reason many sites on the boundaries will still be connected to the network by long baselines (up to 3,000 km), thus reducing the network robustness itself.

In the past years several authors investigated the effect of combining GPS and GLONASS observations for CORS network processing: Bruyninx (2006) assessed the impact of GLONASS for a national mixed-type receiver network and found no evidence that a 15 satellite GLONASS constellation improves the precision of the estimates. Habrich (2009) investigated several processing strategies and also reported no improvement for the repeatability of the coordinates of a regional network. Dach et al. (2009) reviewed the GLONASS-related CODE processing strategy for a global

[1] http://www.ga.gov.au/earth-monitoring/geodesy/asia-pacific-reference-frame.html

A. Nardo (✉) • L. Huisman
Department of Spatial Sciences, Curtin University, Bentley, WA, Australia
e-mail: andrea.nardo@gmail.com

P.J.G. Teunissen
Department of Spatial Sciences, Curtin University, Bentley, WA, Australia

Delft Institute of Earth Observation and Space Systems (DEOS), Delft, The Netherlands

C. Rizos and P. Willis (eds.), *Earth on the Edge: Science for a Sustainable Planet*, International Association of Geodesy Symposia 139, DOI 10.1007/978-3-642-37222-3_31,

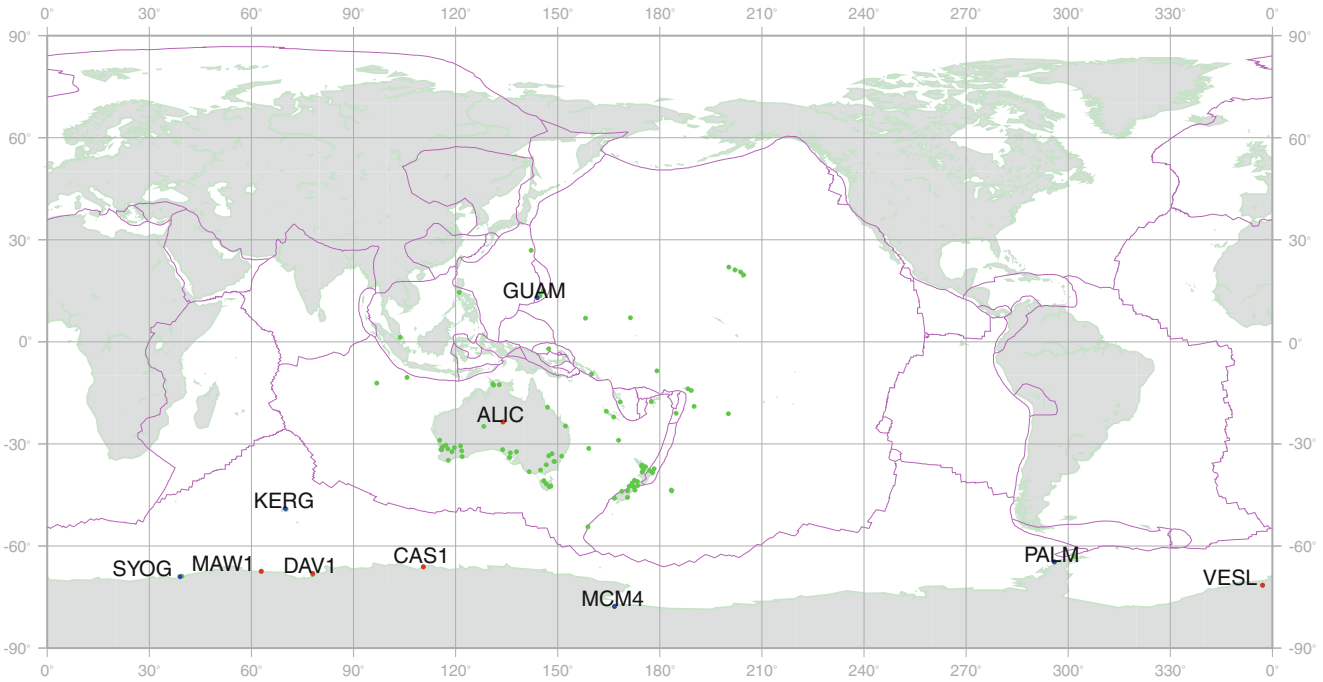

Fig. 1 The cluster of APREF stations processed by CU LAC since Jan 2009. The named stations have been chosen to assess the effect of GLONASS, *blue dots* are the GPS-only stations, *red dots* are the GPS + GLONASSs

network and Dach et al. (2011) investigated the effects of GLONASS-based antenna phase centre corrections. Several authors showed that for 24-h based processing the contribution of GLONASS in terms of precision is marginal.

The additional observations are expected to improve the reliability of the network. Furthermore GLONASS, by virtue of the greater orbit inclination, should provide a better observation geometry, at least for the sites located at high latitude (such as the Antarctica stations). However these benefits seem to be counterbalanced by the poorer accuracy of GLONASS orbits and clock corrections.

The goal of our work is to investigate whether the combined GPS + GLONASS system improves the precision of the estimated coordinates for the APREF network, considering that the GLONASS system has been revitalized the past decade and now its constellation is close to complete (22 satellites active in 2010).

2 Curtin University APREF Local Analysis Centre

Curtin University (CU) has been working as Local Analysis Centre (LAC) for APREF since gps week 1,512 (1 Jan 2009), together with Geoscience Australia (GA), in order to provide weekly coordinates and Zenith Tropospheric Delays (ZTDs) estimates for a sub-network of the APREF. The number of sites of the CU sub-network has been increasing steadily since the beginning of 2009 and currently has grown up to 100. The network size is visualized in Fig. 1, which represents all the stations active from Jan 2009 until April 2011.

2.1 CU Processing Strategy Description

The reprocessing of the CU APREF network was performed by Bernese 5.0 GPS Software (BSW5) on iVEC, the Western Australia's supercomputing facility. Double differenced phase observations were used in a daily batch processing scheme (Beutler et al. 2007). Each daily campaign was processed in parallel, following a strategy sketched in Fig. 2. Such strategy is made of four stages, (1) Data Preparation (data download, reformatting of the files), (2) Data Editing (receivers clock synchronization, outliers and cycle slip detection, estimation of a first approximate solution), (3) Ambiguity Resolution, (4) Final Adjustment.

The GLONASS (IGL) and the GPS (IGS) precise ephemerides were merged in a single file (box MERGE). The receiver clock synchronization was performed by using GPS-only code data (box L3 SPP). This should be regarded as a safe option because sometimes we observed that the receiver clock synchronization (block L3 SPP) was impaired by GLONASS data. For each daily campaign, the baselines were defined to maximize the number of GPS-only observations. The baselines were then saved in the baseline definition file which was also used for the GPS + GLONASS processing of the same daily campaign (box SD).

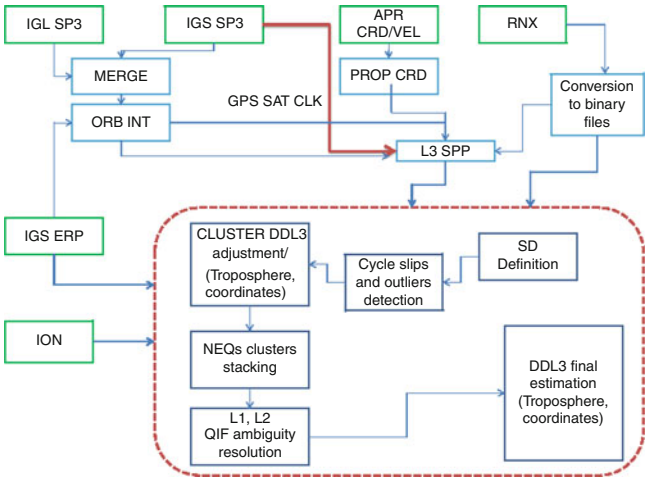

Fig. 2 Processing strategy used for the combined GPS + GLONASS processing: *green boxes* represent the input information, *light blue boxes* point out the main steps of the pre-processing, *dark blue boxes* enclosed by the *dashed line* represent the double difference processing, *blue lines* describe the processing flow

A float double differenced, ionosphere free solution was obtained by processing clusters of five stations individually (box CLUSTER DDL3), and combining the clusters normal equations to compute an approximated network solution (box NEQs clusters stacking). Ambiguities are fixed to integer values through the Quasi Ionosphere Free (QIF) strategy, in which the a-priori part of the ionosphere is provided by the Centre for Orbit DEtermination (CODE) ionospheric maps, while the stochastic single differenced part (between receivers) is constrained to zero (standard deviation = 0.25 cm). Each baseline is processed separately, holding fixed the ZTDs and the coordinates of one station to the values estimated in the float solution. No attempt to estimate GLONASS integer ambiguities was done (box L1, L2 QIF ambiguity resolution) because the suggested Integer Ambiguity Resolution strategy (SIGMA, Beutler et al. 2007) can be applied only for short baselines (20 km).

Finally, after ambiguity resolution, a final double differenced ionosphere free processing is carried out for the entire CU network. Final estimates, based on 180 s sampled data, are the daily coordinates and ZTDs values (2-h sampled) (box DDL3 final estimation).

3 Preliminary Assessment of the Precision of the Estimates for the Daily Processing

The increased number of observations due to the inclusion of GLONASS should result in an improvement of the estimates of the coordinates and the ZTDs, however this improvement is reduced by an increment of the number of parameters to be estimated, mainly the GLONASS float ambiguities.

Table 1 Typical values for the CU network during the first 160 days of 2010

Total num. of receivers	84
Num. of observed GPS satellites	31
Fract. of fixed GPS amb. per day	0.83
Ratio between GPS-only and GPS + GLO rec.	0.6
Num. of ZTDs values per rec. per day	13
Average num. of epochs per sat. pass (180 s sampl.rate)	130
Average num. of cycle slips per pass	3

For a full-rank system of observation equations, redundancy (degrees of freedom) is defined as the number of observations minus the number of unknowns. We define the fractional increment of the redundancy as:

$$dr = \frac{r_{GPS+GLO} - r_{GPS}}{r_{GPS}} \tag{1}$$

where r_{GPS} is the redundancy of the GPS-only model and $r_{GPS+GLO}$ is the redundancy of the GPS + GLONASS model. As an example we consider the CU network in the first 160 days of 2010. Typical values for the configuration of the network in that period are listed in Table 1.

During this interval the number of GLONASS satellites n_{GLO} processed by Bernese 5.0 increased from 15 to 20. The quantity dr computed at the beginning of 2010 (15 satellites) is:

$$dr_{15} = 0.21 \tag{2}$$

and at the end of the considered period (20 satellites):

$$dr_{20} = 0.32. \tag{3}$$

Despite the increase of the number of the ambiguities, there is still a sensible increase of the redundancy (up to 32 %). The redundancy, as well as the derived quantity dr, is mainly dependent on the number of satellites. By taking into account the ratio between the number of GLONASS and GPS satellites, we can derive an approximated expression for the improvement of the coordinates precision. We consider a double-differenced ionosphere free observation system. Such a system is of full rank and *partitioned* Teunissen (2009). The VCV matrix of the ZTDs and baselines for the GPS + GLONASS processing is related to the GPS and GLONASS counterparts by the following relation:

$$Q_{GPS+GLO} = Q_{GPS} - Q_{GPS}\left(Q_{GPS} + Q_{GLO}\right)^{-1} Q_{GPS}. \tag{4}$$

If the GPS and GLONASS functional and stochastic models were equivalent, the VCV matrices would mainly be driven by the number of observations provided by each system. We thus assume that the matrix Q_{GLO} is obtained from the Q_{GPS} by means of a multiplicative factor Bruyninx (2006):

$$Q_{GLO} = \alpha Q_{GPS}, \tag{5}$$

substitution of (5) into (4) gives:

$$Q_{GPS+GLO} = \frac{\alpha}{1+\alpha} Q_{GPS}. \tag{6}$$

We also assume that such factor is the ratio between the number of GPS and the number of GLONASS satellites. In the best case, at the end of the reprocessing (16th April 2011), observations from 22 GLONASS satellites and 31 GPSs have been processed, so the ratio is:

$$\alpha = 31/22 = 1.40 \tag{7}$$

and from (6):

$$Q_{GPS+GLO} \approx 0.58 Q_{GPS}. \tag{8}$$

In the worst case of the considered time interval (1st Jan 2009), 16 GLONASS and 31 GPS satellites have been processed, and we get:

$$Q_{GPS+GLO} \approx 0.66 Q_{GPS}. \tag{9}$$

The standard deviations scale as $\sqrt{0.58} = 0.76$ and $\sqrt{0.66} = 0.81$, respectively, meaning that the expected improvement due to the increased number of observations is 24 % at the end of the reprocessing and 19 % at the beginning. Considering that the usual repeatabilities values for the coordinates in the APREF case are $\approx$ 3 mm for the horizontal coordinates and $\approx$ 7 mm for the height, we expect that the improvement will be sub-millimetric.

4 Long Term Processing

In this section we compare the estimates of the coordinates generated by the two different daily processings (GPS-only and GPS + GLONASS), aiming at evaluating the possible precision improvement (i.e. the standard deviations of the coordinates). We report results of stations located in Antarctica (seven stations in total), in order to emphasize the possible effect of the better observation geometry due to GLONASS orbit inclination at high latitudes. For comparison we also report the results from three more stations, one located on the Australian continent (ALIC), and the other two on the boundaries of the network (GUAM and KERG). The location of the sites are shown in Fig. 1 (red and blue dots, representing the GPS + GLONASS and the GPS-only stations, respectively).

4.1 Time Series Generation

Coordinate time series obtained from the daily solutions are used to estimate the precision (repeatability) of the coordinates. CATREF software (Altamimi et al. 2007) has been used for the time series stacking, as its mathematical model allows to solve for both the coordinates and the reference frame parameters, thus removing the effect due to the variability of the reference frame definition from the coordinates time series.

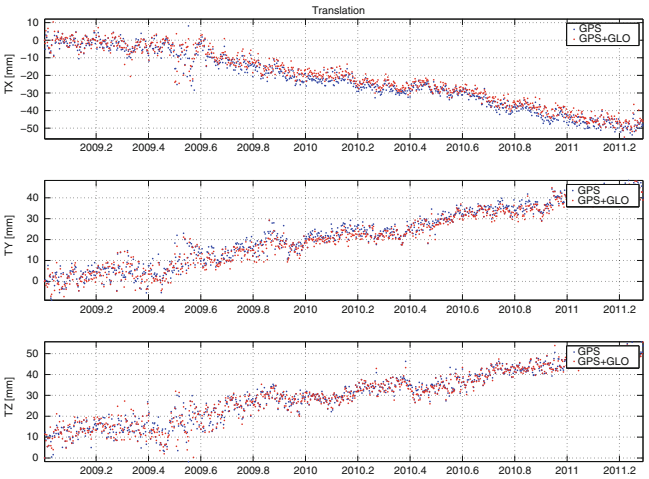

Fig. 3 Evolution in time of the translation parameters, GPS (*blue dots*), GPS + GLONASS (*red dots*)

4.2 CATREF Functional Model

The estimates of coordinates and velocities stored in the SINEX files, together with their VCV matrix, can be used as observations in a further least squares adjustment after removal of the original constraints. The CATREF functional model is based on (linearized) coordinate- and velocity transformations between two or more reference frames. Assuming that each set of coordinates (i.e. each SINEX file) defines a different reference frame and taking into account both the coordinates and the velocities of the sites, the software estimates the 14 Helmert parameters (translation, rotation, scale and their time derivatives) between the two reference frames as well as the coordinates and the velocities in a combined reference frame. The time-dependence of the Helmert parameters can be assumed linear (if an appropriate set of solution numbers has been defined for each site, based upon a preliminary analysis of each time series), as we see in Fig. 3. The (linearized) observation equations read as:

$$\begin{aligned} X_S^i &= X_C^i + (t_S^i - t_0)\dot{X}_C^i + T_k + D_k X_C^i + R_k X_C^i \\ &\quad + (t_S^i - t_k)[\dot{T}_k + \dot{D}_k X_C^i] \\ \dot{X}_S^i &= \dot{X}_C^i + \dot{T}_k + \dot{D}_k X_C^i + \dot{R}_k X_C^i \end{aligned} \tag{10}$$

where X_S^i and $\dot{X}_S^i$ are the coordinates and the velocity for each individual solution S and for each station i at

epoch t_S^i in a given Terrestrial Reference Frame (TRF) k, X_C^i and $\dot{X}_C^i$ are the coordinates and the velocity in the combined reference frame, t_k is the epoch each individual TRF refers to, T_k, D_k, R_k are the translation, rotation and scale parameters and $\dot{T}_k$, $\dot{D}_k$, $\dot{R}_k$ their time derivatives and t_0 is a reference epoch. Because of a rank defect of 14 (7, if only coordinates are considered) in the design matrix, the solution of the normal equations is not unique. One particular solution can be selected by choosing an appropriate *S-basis* Teunissen (1985) which results in the definition of a minimum number of additional conditions, equal to the rank defect. As many choices for such conditions are possible, we have chosen the ones for expressing the solution in ITRF2005. Let X_R and X_C be the external ITRF2005 and the combined solution, respectively. The transformation between the two frames is defined as (Altamimi et al. 2007):

$$X_R - X_C = A\theta \tag{11}$$

where $A = [X_0^i]_\times$, X_0^i are the approximated values used in the linearization and θ are the transformation parameters. In order to express the combined solution in the ITRF2005 the transformation parameters must be minimized. Such a condition leads to the following constraint equations (Altamimi et al. 2007):

$$(A^T A)^{-1} A^T (X_R - X_C) = 0. \tag{12}$$

Equation (12) is added to the normal equation system associated with (10) to complete the rank defect and express the solution in an external reference frame.

4.3 Functional and Stochastic Model for the Time Series of the Coordinates

The output of CATREF are the residuals of the daily ITRF2005-aligned coordinates computed w.r.t the combined solution, for each site, and expressed in the North, East and Up frame (NEU). The functional model for a single component i ($i = n, e, u$) of each NEU time series can be written as (Amiri-Simkooei 2009) a superposition of a straight line, accounting for the secular motion, and sinusoidal terms representing the annual periodic effect, complemented with a piece-wise function to absorb discontinuities (Fig. 4). Let $\hat{E}_r$ be the matrix the columns of which represent the NEU residuals w.r.t. the model, then an estimate $\hat{\Sigma}$ of the VCV empirical matrix for the coordinates can be written as (Amiri-Simkooei 2009):

$$\hat{\Sigma} = \frac{\hat{E}_r^T \hat{E}_r}{m - n} \tag{13}$$

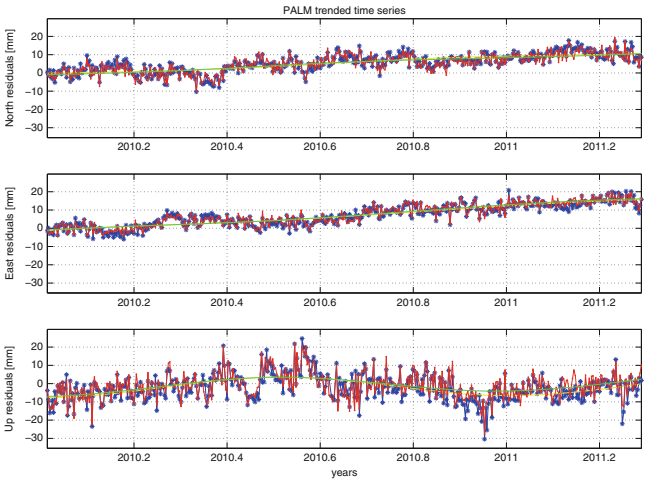

Fig. 4 Example of a time series showing secular and periodic motion (PALM station), GPS (*blue line*), GPS + GLONASS (*red line*), *green solid line* is the fitted model

where m is the number of observations and n is the number of estimated parameters. Being $\hat{\Sigma}$ an estimate, we can also compute the uncertainties of its elements. The elements $\hat{\Sigma}$ matrix can be collected in the vector $\left(\hat{\sigma}_{ij}\ \hat{\sigma}_{ii}\ \hat{\sigma}_{jj}\right)^T{}_{i,j=n,e,u}$ and the VCV matrix of this vector can be written as (Amiri-Simkooei 2009):

$$Q_{\hat{\sigma}}^{ij} = \frac{1}{m-n} \begin{pmatrix} \sigma_{ii}\sigma_{ij} + \sigma_{ij}^2 & 2\sigma_{ii}\sigma_{ij} & 2\sigma_{jj}\sigma_{ij} \\ 2\sigma_{ii}\sigma_{ij} & 2\sigma_{ii}^2 & 2\sigma_{ij}^2 \\ 2\sigma_{jj}\sigma_{ij} & 2\sigma_{ij}^2 & 2\sigma_{jj}^2 \end{pmatrix} \tag{14}$$

where $i, j = n, e, u$. From (14) we have:

$$\sigma_{\hat{\sigma}_{ii}}^2 = \frac{1}{m-n} 2\hat{\sigma}_{ii}^2,\ i = n, e, u \tag{15}$$

The precision of the standard deviations $\hat{\sigma}_n = \sqrt{\hat{\sigma}_{nn}}$, $\hat{\sigma}_e = \sqrt{\hat{\sigma}_{ee}}$ and $\hat{\sigma}_u = \sqrt{\hat{\sigma}_{uu}}$ is computed by applying the error propagation law after linearization (Tables 2 and 3). We have:

$$\sigma_{\hat{\sigma}_n} \approx \frac{\sigma_{\hat{\sigma}_{nn}}}{2\hat{\sigma}_n} \qquad \sigma_{\hat{\sigma}_e} \approx \frac{\sigma_{\hat{\sigma}_{ee}}}{2\hat{\sigma}_e} \qquad \sigma_{\hat{\sigma}_u} \approx \frac{\sigma_{\hat{\sigma}_{uu}}}{2\hat{\sigma}_u}. \tag{16}$$

4.4 Effect on the Empirical Errors

For the considered sites the empirical VCV matrices $\hat{\Sigma}$ have been computed by means of (13) and the corresponding standard deviations have been computed by using (16). In order to evaluate the improvement of the GPS + GLONASS processing w.r.t. the GPS-only, we define the following non-dimensional quantity:

$$F_i = 1 - \frac{\hat{\sigma}_i^{GPS+GLO}}{\hat{\sigma}_i^{GPS}},\ i = n, e, u \tag{17}$$

Table 2 Standard deviations with their precision $\sigma_{\hat{\sigma}_n}$, $\sigma_{\hat{\sigma}_e}$, $\sigma_{\hat{\sigma}_u}$, for the considered stations (expressed in *mm*), GPS-only case

Site	$\hat{\sigma}_n$	$\hat{\sigma}_e$	$\hat{\sigma}_u$
MCM4	2.55 ± 0.02	2.48 ± 0.02	8.15 ± 0.02
VESL	3.06 ± 0.03	3.23 ± 0.03	5.82 ± 0.03
SYOG	2.97 ± 0.03	3.27 ± 0.03	4.87 ± 0.03
DAV1	2.70 ± 0.03	2.99 ± 0.03	4.66 ± 0.03
MAW1	2.82 ± 0.03	2.98 ± 0.03	4.85 ± 0.03
CAS1	3.00 ± 0.03	3.09 ± 0.03	5.07 ± 0.03
PALM	4.30 ± 0.03	3.49 ± 0.03	7.17 ± 0.03
KERG	3.09 ± 0.03	3.29 ± 0.03	8.30 ± 0.03
ALIC	1.30 ± 0.03	1.28 ± 0.03	7.13 ± 0.03
GUAM	2.87 ± 0.03	4.38 ± 0.03	10.86 ± 0.03

Table 3 Standard deviations with their precision $\sigma_{\hat{\sigma}_n}$, $\sigma_{\hat{\sigma}_e}$, $\sigma_{\hat{\sigma}_u}$, for the considered stations (expressed in *mm*), GPS + GLONASS case

Site	$\hat{\sigma}_n$	$\hat{\sigma}_e$	$\hat{\sigma}_u$
MCM4	2.48 ± 0.02	2.38 ± 0.02	8.37 ± 0.02
VESL	3.23 ± 0.03	3.11 ± 0.03	5.82 ± 0.03
SYOG	3.01 ± 0.03	3.26 ± 0.03	4.96 ± 0.03
DAV1	2.62 ± 0.03	2.89 ± 0.03	4.73 ± 0.03
MAW1	2.76 ± 0.03	2.99 ± 0.03	5.01 ± 0.03
CAS1	2.54 ± 0.03	2.47 ± 0.03	4.56 ± 0.03
PALM	4.42 ± 0.03	3.43 ± 0.03	7.09 ± 0.03
KERG	3.82 ± 0.03	3.33 ± 0.03	3.91 ± 0.03
ALIC	1.28 ± 0.03	1.25 ± 0.03	5.68 ± 0.03
GUAM	2.83 ± 0.03	4.52 ± 0.03	10.81 ± 0.03

Table 4 Fractional improvements, time interval (T) of the time series and number of discontinuities (n_d), stations are sorted by latitude, being MCM4 the southernmost

Site	F_n	F_e	F_u	T[y]	n_d
MCM4	0.03	−0.02	−0.03	2.2850	0
VESL	−0.06	0.01	−0.08	2.2820	0
SYOG	−0.01	0.00	−0.02	2.2820	0
DAV1	0.03	0.04	−0.02	2.2140	1
MAW1	0.02	0.00	−0.03	2.2710	0
CAS1	0.03	0.12	0.02	2.2850	0
PALM	−0.03	0.01	0.01	2.2820	0
KERG	0.02	−0.01	0.00	2.2850	0
ALIC	0.01	0.20	0.19	2.2850	1
GUAM	0.01	−0.03	0.00	2.2850	1

where $\hat{\sigma}_i^{GPS}$ is the standard deviation of the i-th component, as estimated by the GPS-only processing, and $\hat{\sigma}_i^{GPS+GLO}$ is the corresponding standard deviation from the GPS + GLONASS processing. Quantity F_i is positive and smaller than 1 if the additional GLONASS observations improve the estimate of the unknown parameters, otherwise it is negative. Table 4 summarizes the results of the comparison: as we can see the GLONASS system does not give any remarkable improvement, also there is no appreciable effect dependent on the latitude of the sites of the stations.

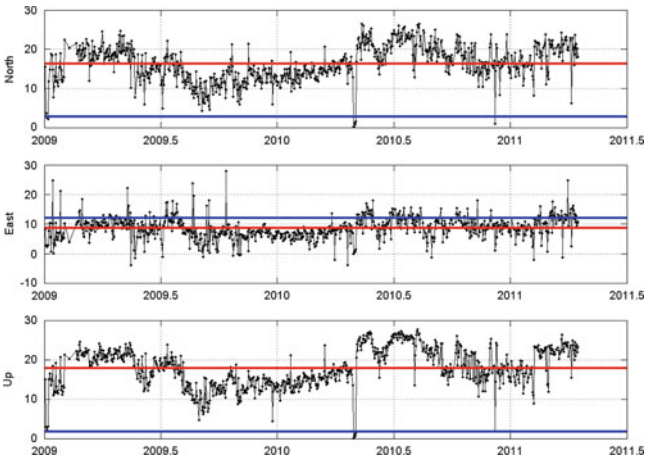

Fig. 5 CAS1, the non-dimensional quantities $F_{i,snx}$ (*black line*), $\overline{F}_{i,snx}$ (*red line*), F_i (*blue line*), (17). Vertical scale is multiplied by 100, horizontal scale is in years

4.5 Effect on the Formal Errors

For the considered sites the coordinate VCV matrices have been extracted from the daily SINEX files and transformed in the NEU reference system. The improvement of the formal errors is defined by the fractional decrease of the standard deviation $F_{i,snx}$, in a way similar to (17). In order to compare quantity $F_{i,snx}$ with F_i, the mean value $\overline{F}_{i,snx}$ has been computed. The plot of $F_{i,snx}$ and $\overline{F}_{i,snx}$ for the site CAS1 (black and red lines, respectively) and the corresponding F_i value (blue line) are shown in Fig. 5. CAS1 is the station that shows the best improvement related to the introduction of GLONASS data. As we can see the improvement derived from the formal VCV matrices agrees quite well with the rough estimate given by (9). Nevertheless the formal VCV matrix is not in agreement with the empirical $\hat{\Sigma}$, as Fig. 6 shows. The blue and red confidence ellipses (95 %) are the empirical ones computed on the basis of the GPS-only and GPS + GLONASS processing, while the black and the green ellipses are the ones derived from formal daily VCV matrices. As a comparison, Fig. 7 shows the corresponding empirical error ellipses freed of any reference frame effect.

4.5.1 Effect on the Reference Frame

Each daily solution is aligned to the ITRF2005 reference frame by means of constraints imposed on translation parameters. As the subset of stations chosen to define the reference changes from day to day, and the time series of the transformation parameters show a linear trend due to the plate motion, we can identify the scattering around the

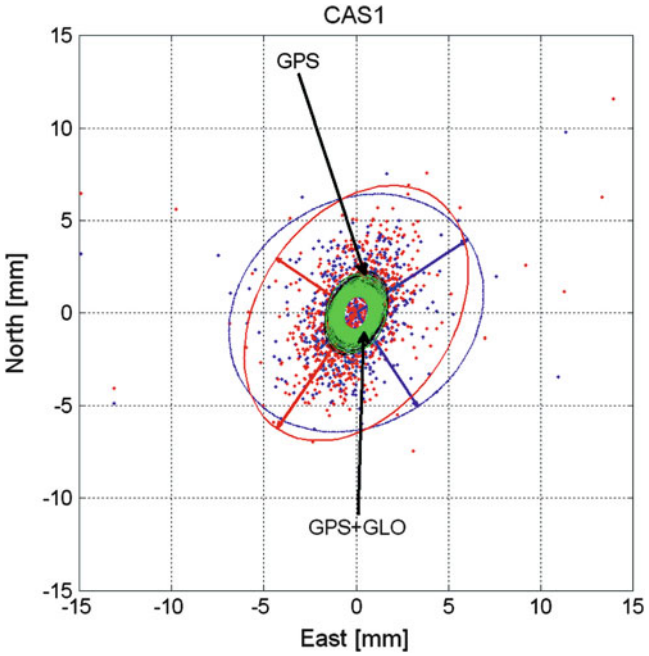

Fig. 6 CAS1 scatterplot derived by SINEX files, *black and green ellipse* (95 %) computed on the basis of the formal VCV matrix

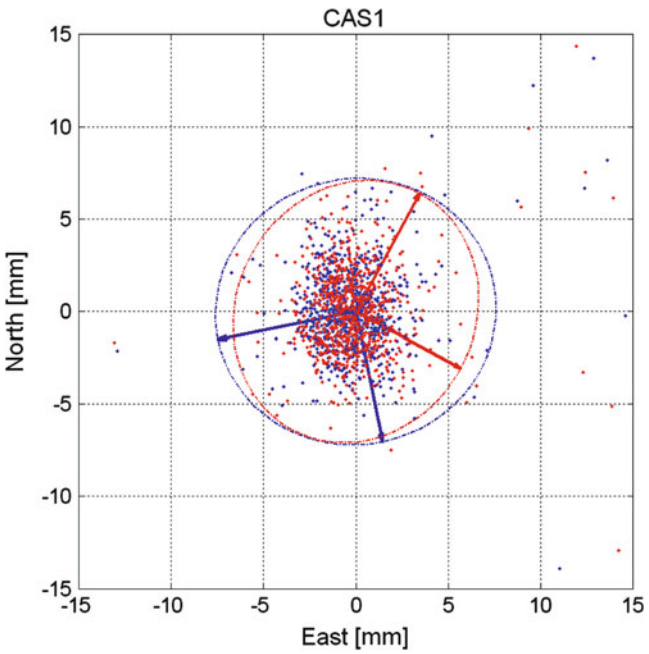

Fig. 7 CAS1 scatterplot derived by CATREF residuals. The reference frame effects have been absorbed by the reference frame parameters, therefore the error ellipses (95 %) are less elongated than their counterparts in Fig. 6

best fit line as the indirect contribution of the processing strategy. From the results of the previous sections we do not expect any appreciable effect: this is confirmed by Table 5 which shows the standard deviations of the reference frame parameters computed by means of (13).

Table 5 Standard deviations of the residuals of the reference frame parameters

	GPS	GPS + GLO
$\sigma_{\hat{e}\hat{e}}\, T_x$ [mm]	3.6	3.4
$\sigma_{\hat{e}\hat{e}}\, T_y$ [mm]	3.1	3.2
$\sigma_{\hat{e}\hat{e}}\, T_z$ [mm]	3.5	3.7
$\sigma_{\hat{e}\hat{e}}\, R_x$ [mas]	0.08	0.08
$\sigma_{\hat{e}\hat{e}}\, R_y$ [mas]	0.12	0.12
$\sigma_{\hat{e}\hat{e}}\, R_z$ [mas]	0.09	0.09
$\sigma_{\hat{e}\hat{e}}\, D$ [ppb]	2.1	2.1

5 Conclusion

This 2.5 years-long investigation, based on a daily analysis, aimed at assessing GLONASS impact for long term geodynamic studies and reference frame maintenance. In such a case the improvement of the formal precision of the coordinates for some of the sites on the boundary of the network has been achieved in accordance with (6). Also, the reference frame stability is virtually not affected by the additional GLONASS observations.

The fact that the formal errors are mainly in agreement with (8) and (9), while the empirical errors are not (as we see in Fig. 5), might point out to the presence of mismodelling. According to Dach et al. (2011) the PCV based on GPS-only can cause a mean difference of up to 1 cm in the modeling of the L3 phase observable for the GLONASS (when compared to the GLONASS-specific PCVs), which is partly absorbed by the GPS-GLONASS system bias, furthermore, the error of the GLONASS orbit should be taken into account because it is still twice the corresponding error for the GPS, causing an error of 4 mm on baselines of 2,000 km (as given by the approximation $\Delta x = \frac{l}{d}\Delta X$, where Δx is the baseline error, l is the baseline length, d is distance receivers-satellites and ΔX is the orbit error, Beutler et al. (2007)).

We observed that the stochastic model is not fully adequate even for the GPS-only processing, resulting in over-optimistic formal precision for the coordinates, as shown in Fig. 6.

Even if there is still room for the improvement of the functional model, a rough estimate based on the number of observations shows that the improvement, for a GPS + GLONASS system, will be sub-millimetric. In a near future scenario, for example, when the number of visible GPS satellites will equal the number of GLONASS (24 for each constellation), the relative improvement of the precision of the daily estimates of the coordinates, as computed by (6), will still be around 30 %.

Acknowledgements The work was supported by iVEC through the use of advanced computing resources located at iVEC@MURDOCH. Part of the presented work has been done in the framework of the

Australian Space Research Project (ASRP2, Platform Technologies for Space, Atmosphere and Climate). The third author is the recipient of an Australian Research Council Federation Fellowship (project number FF0883188): this support is gratefully acknowledged.

References

Altamimi Z, Collilieux X, Legrande J (2007) ITRF2005: a new release of the International Terrestrial Reference Frame based on time series of station positions and Earth orientation parameters. J Geophys Res 112

Amiri-Simkooei AR (2009) Noise in multivariate GPS position time series. J Geodes 83:175–187

Beutler G, Bock H, Fridez P, Gade A, Hugentobler U, Dach R, Jaggi A, Meindl M, Mervart L, Prange L, Schaer S, Springer T, Urschl C, Walser P (2007) Bernese 5 GPS Software user manual. Astronomical Institute, University of Bern

Bruyninx C (2006) Comparing gps-only with GPS + GLONASS positioning in a regional permanent GNSS network. GPS Solut 11:97–106

Dach R, Brockmann E, Schaer S, Meindl M, Prange L, Bock H, Jaggi A, Ostini L (2009) GNSS processing at code: status report. J Geodes 83:353–365

Dach R, Schmid R, Schmitz M, Thaller D, Schaer S, Lutz S, Steigenberger P, Wubbena G, Beutler G (2011) Improved antenna phase centre models for GLONASS. GPS Solut 15:49–65

Habrich H (2009) Evaluation of analysis options for GLONASS observations in regional GNSS networks. Geodetic Ref Frames 134:121–129

Teunissen PJG (1985) Zero order design: generalized inverses, adjustment, the datum problem and S-transformations. In: Grafarend EK, Sanso F (eds) Optimization and design of geodetic networks. Springer, London

Teunissen PJG (2009) Adjustment theory: an introduction. Delft University Press, Delft